III. Magnetospheric observations and theory

A. Event studies and special locations

#. Tripolar Solitary Structures

The survey by Pickett et al. (2004b) showed that tripolar pulse (two positive peaks and one negative peak, or vise versa) solitary structures are detected everywhere that the more typical bipolar pulse type is detected with the same types of characteristics. Similar tripolar pulses have been detected by the Wind spacecraft in the solar wind (Mangeney et al., 1999) and in Short Large Amplitude Magnetic Structures upstream of the Earth's quasi-parallel bow shock (Goldstein et al., 2005). The tripolar solitary structures observed by Cluster in the auroral zone at 4.5-6.5 R_E as the spacecraft crossed field lines that map to the auroral acceleration region were studied in more detail by Pickett et al. (2004a). Their study found that there was a small measurable potential change, up to 0.5 V, across the tripolar pulses, whereas there was no measurable change across the bipolar pulses. This led Pickett et al. (2004a) to conclude that the tripolar solitary structures were weak double layers. Further, they presented an example of a pair of tripolar structures on one spacecraft being detected by a second Cluster spacecraft (correlation coefficient of 0.78) separated by 56 km along B and 251 km across B (see Figure 1). The lag time from the first to the second spacecraft was 0.02 s, resulting in a velocity of 2800 km/s, a parallel size of 4.5 km, and a perpendicular size of at least 251 km. The authors pointed out that they were unable to find any significant correlations of propagation of the bipolar type pulses from one spacecraft to another. The generally poor results for this correlation study imply that the spacecraft are probably too far apart and that this, combined with evolution of the structures (growing, decaying) over such short time scales makes it nearly impossible to identify the same structures on more than one spacecraft.

Pickett et al. (2004a) suggest that the same types of mechanisms that generate the bipolar solitary waves may be behind the generation of the tripolar ones as well since their characteristics are similar. They suggested the usual types of beam instabilities that lead to particle trapping, as well as spontaneous generation out of turbulence as possible generation mechanism. In the case of particle trapping, Pickett al. (2004a) noted that for the tripolar pulses, because their potential signature has a potential dip (traps ions) and a hump (traps electrons), it would require both trapped electrons and trapped ions to be sustained.

B. Statistics and Surveys

1. Cusp/Plasma Sheet Statistics from Polar PWI

The Polar spacecraft Plasma Wave Instrument (PWI) (Gurnett et al., 1995) was used to carry out a statistical study of the properties of the coherent structures (solitary waves) observed in the cusp and plasma sheet (Franz, 2000). For this study, waveform data from 19 different Polar orbits spanning in time from June 1996 to May 1997 were analyzed.

The Polar Hydra (Scudder, et al., 1995) particle data were used to determine when the spacecraft was in the cusp. The interferometry mode of the PWI waveform receiver (see Franz et al, 1998, 2000) was used to make the measurements, thus obtaining the ability to obtain the velocity and parallel size of the structures, in addition to their potential amplitudes. In this particular mode, the data were telemetered directly to the ground, providing 190,900 12-bit samples in each snapshot with a 14 μs sample period. One snapshot was obtained every 9.2 seconds, with the length of each snapshot depending on the number of channels selected. In interferometry mode typically 2 or 3 channels were selected providing simultaneous measurements of the ac electric field in a 25 kHz bandwidth (50 Hz – 25 kHz) . If only two channels were selected, both were taken along the interferometer axis (each interferometer antenna 50m long) in the spacecraft spin plane. If three simultaneous measurements were obtained, these consisted of the two interferometer measurements plus a third measurement consisting of the average potential between the two spheres of the other spin plane antenna (132m length), which is perpendicular to the interferometer axis. An automatic algorithm was used to detect the coherent structures that was optimized for not detecting false positives. This resulted in the program only detecting on the order of 10-20 percent of the structures that were observed, and somewhat biasing the detections to structures with higher amplitudes. In order to keep the error in the velocity measurement to a minimum, the interferometer axis was required to be within 20º of **B**, and structures which had “clipped” electric field waveforms were discarded.

Structure Properties

Table 1, which is adapted from Franz (2000), presents a comparison of the properties of the coherent structures that were automatically detected during cusp (6-9 R_E) and plasma sheet crossings (4-6 R_E) during the period described above. The primary differences between the two regions were found to be as follows: 1) the velocities of the plasma sheet structures are generally much greater than those observed in the cusp; 2) the parallel sizes of the plasma sheet structures are typically larger than those observed in the cusp; 3) the cusp structures are almost always larger than the Debye length while the plasma sheet ones are not; and 4) the shape of the cusp structures are more pancake-like, while those in the plasma sheet are more spherical, as was the case for the structures observed in the auroral acceleration region (Ergun et al., 1998). The structures share some common properties, though, in that all of them have potential amplitudes much less than the electron thermal energy and their velocities are almost always greater than theory would predict for the velocity of ion acoustic solitons. Thus, Franz (2000) concluded that the structures were probably not ion acoustic solitons.

Trends

Franz (2000) also investigated the properties of the solitary structures just described with respect to other physical plasma parameters in order to look for trends in the data. Scatter plots were produced of the parallel size of the structures vs. the Debye length, the electron thermal velocity and the electron thermal energy. None of these showed any strong correlation for either the cusp or plasma sheet regions, although there was a weak correlation for both regions of the parallel scale length with the Debye length and electron thermal velocity, this being a slight trend for the parallel scale length to increase with increasing Debye length and electron thermal velocity. A more enlightening outcome was achieved when comparing various properties of the structures with each other. Figure 2 is a scatter plot of the cusp structures showing the normalized velocity vs. the normalized scale size in the top panel, the normalized amplitude vs. the scale size in the middle panel and the normalized amplitude vs. the normalized velocity in the bottom panel. These results show that the larger scale structures and the larger amplitude structures tend to have larger velocities. Furthermore, the middle panel of Figure 2 shows a trend of the larger amplitude structures to have larger scale sizes, which is opposite to the trend predicted by soliton theory. The correlation coefficient for all panels is no higher than 0.4. Thus, these results show a general trend but not a strong correlation. Similar results to those in Figure 2 are found for the structures detected in the plasma sheet. Here again the trends for larger scale and larger amplitude structures to have larger velocities and for the scale size to increase as the amplitude increases are but weak correlations. Based on these trends, Franz (2000) concluded that the structures were probably not classical solitons.

Although Franz (2000) uncovered a general trend of structure scale size to increase with increasing amplitude, he did not attempt to understand why this trend existed. Chen and Parks (2002a,b), Muschietti et al. (2002) and Chen et al. (2004) shed light on these trends through theoretical studies of Bernstein-Greene-Kruskal (BGK) solitary waves. They found that the key property of BGK solitary structures is that their widths and amplitudes are constrained by inequalities. Therefore, a large range of electric field amplitudes and widths is expected. Further these inequalities show that the solitary structure amplitudes will increase as the structure width increases. This could, then, potentially explain the great scatter in Figure 2 and the low correlation coefficient, but allow for the general trend of increasing scale size with increasing amplitude. Further studies of this BGK theory inequality as it specifically relates to the Franz (2000) statistics are continuing.

Generation Mechanism

Franz (2000) suggested a possible generation mechanism for the structures observed in the high altitude cusp. Observations in this region indicated that low frequency (~100-300 Hz) electromagnetic whistler mode waves were involved in the generation of higher frequency (3-10+ kHz), parallel propagating electrostatic waves. Franz (2000) speculated that these electrostatic waves may evolve into the coherent structures that are observed. Pickett et al. (2001) explored the generation of these electrostatic waves further and concluded that they were created by a type of two-stream instability, namely the resistive medium instability. They did not attempt to explain how these waves evolve into solitary structures.

Interpretation

Franz (2000) interpreted the solitary structures that were observed by Polar PWI in the high altitude cusp and plasma sheet regions as electron phase space holes. He came to this conclusion by noting that the structures were inconsistent with a soliton interpretation due to the direct relationship between increasing width with increasing amplitude. Further, he compared the observations with the electron phase space hole model of Krasovsky et al. (1997). The Krasovsky et al. (1997) model is one-dimensional theory of an equilibrium electron phase-space hole. Their theory considers a Gaussian-shaped potential in a Maxwellian plasma, and neglects ion effects. The requirement that the distribution function is non-negative leads to a minimum allowed scale size as a function of the amplitude and velocity of the structure. This minimum scale size is the primary theoretically-predicted quantity that Franz (2000) compared with the Polar data. Although the Krasovsky, et al. (1997) model required that the size of electron holes had to be many Debye lengths, Franz (2000) found that the structures observed in the cusp and plasma sheet by Polar PWI, with sizes from subDebye scales to a few or several Debye lengths, were generally consistent with the model. Since the completion of the Franz (2000) study, Chen and Parks (2002b) and Chen et al. (2004) have specifically pointed out and emphasized that the theory of BGK solitary waves allows subDebye scale characteristics of electron (and ion) holes.

Franz (2000) further noted that if the work of Dupree (1982) was correct in that phase-space holes are the most probable fluctuations in a plasma, then it is likely that many different types of fluctuations eventually evolve into such structures. Finally, Franz (2000) and Franz et al. (2000) demonstrated that $L_{//}/L_{\perp}$ is small in regions of small Ω_e/ω_p ($\sim \lambda_D/\rho_e$ for Polar), indicating that the structures are quite oblate with $L_{//} < L_{\perp}$.

2. Survey of Solitary Structures from the Near-Earth Plasma Sheet/Auroral Zone to the Solar Wind

Data from the Wideband (WBD) plasma wave receiver of the Cluster mission were used by Pickett et al. (2004b) to carry out a survey of the solitary electrostatic structures observed in all regions from the near-Earth plasma sheet/auroral zone at about 5 R_E out to 19.5 R_E in the solar wind. The WBD instrument detects ac electric field waveforms in the spin plane along only one antenna (axis), measuring the average potential between the two spheres of that antenna. WBD does not have the capability of making measurements in an interferometry mode. Thus, it is not possible to determine the velocity or size of the structures on just one Cluster spacecraft (using two of the Cluster spacecraft as an interferometer to detect the same structure as it propagates from one spacecraft to the other has met with very limited results thus far). Pickett et al. (2004b) characterized the solitary structures by their amplitudes and time durations. They were further classified into two basic categories, the usual bipolar pulse type of structure that has one positive peak and one negative peak, and the tripolar pulse that has two positive peaks and one negative peak, or vise versa. The occurrence rate of the tripolar pulses was found to be about 1/10 that of the bipolar pulses in most regions.

The primary result of the Pickett et al. (2004b) solitary structure survey using Cluster WBD data was that there is a broad range of electric field amplitudes at any specific magnetic field strength, and there is a general trend for the electric field amplitudes to increase as the strength of the magnetic field increases over a range of 5 to 500 nT as shown in Figure 3. This result held true for the bipolar solitary structures as well as the tripolar structures, suggesting that both types of structures are generated by similar mechanisms. One possible explanation was put forth by Pickett et al. (2004b) for the relationship of the amplitude to the magnetic field strength. Here again the explanation relied on the structures being BGK mode solitary waves and the stability requirement associated with this mode of solitary wave (Chen and Parks, 2002a,b; Chen et al., 2004). The Cluster survey found no relationship between the time duration of the solitary waves and the magnetic field strength. It did find, however, that the time duration of the solitary waves, both bipolar and tripolar, were much shorter in the magnetosheath ($\Delta t \sim$ several tens of microseconds) than in all other areas sampled by Cluster ($\Delta t \sim$ few milliseconds). This result seemed to point out that the magnetosheath structures come from a different class (different generation mechanism) than all those found in other regions, requiring further research into this surprising result.

IV Magnetosheath Observations

An initial study of solitary structures observed in Earth's magnetosheath was carried out by Pickett et al. (2003) using Cluster WBD plasma wave data. Because the time durations of the structures in the magnetosheath are very short (several 10s of microseconds), a wide bandwidth is required to detect them. The Cluster WBD receiver is particularly suited for this purpose since it has 3 bandwidths available, 9.5 kHz, 19 kHz and 77 kHz. Only the 77 kHz bandwidth filter is capable of detecting the short duration structures in the magnetosheath, whereas for almost all other regions included in the Pickett et al. (2004b) survey, the 9.5 kHz bandwidth was sufficient. Pickett et al. (2003) found that broadband features seen in the spectrograms produced by performing an FFT on the waveform data from the magnetosheath on two Cluster spacecraft separated by 750 km had similar profiles in terms of onset times, frequency extent, intensity and termination. The broadband features in this case were the result of the FFT rendering of the pulses associated with the solitary structures. The similar spectral profiles on the two Cluster spacecraft implied that the generation region of the solitary structures was very large, perhaps located at the bow shock or associated with the bow shock.

A follow-up study on the generation of the solitary structures observed in the magnetosheath was conducted by Pickett et al. (2005). Through case studies using Cluster data, they showed that the amplitudes and time durations of the structures do not vary from the bow shock to the magnetopause (see Figure 4). Had the bow shock been the location of the generation of the solitary structures which then propagated down stream in the magnetosheath, Pickett et al. (2005) would have expected a change in the amplitudes, in particular, with a decrease in this parameter being most likely the further from the bow shock. The lack of a trend in either the amplitude or time duration suggests a local generation mechanism in the magnetosheath. Counterstreaming electrons were found in all cases where solitary structures were observed, suggesting a generation mechanism involving electrons, the two-stream instability being the most likely. The time durations of the solitary structures also suggest that electrons are involved since the time durations of the pulses are on the order of an electron plasma period or slightly larger. Ions were ruled out as the primary driver behind the generation of the solitary structures since Pickett et al. (2005) found no change in the characteristics of the structures with ion velocity. Finally, they also found no preference for either the generation of the structures or changes in their characteristics with the type of bow shock (quasi-parallel or quasi-perpendicular) which Cluster was subject to in the magnetosheath. Thus, further work is required in order to look at other parameters of interest that affect the magnetosheath, such as plasma beta. In addition, modeling needs to be carried out to test whether the counterstreaming electrons are sufficient to create the solitary structures.

Prior to Cluster, observations of solitary structures in the magnetosheath have primarily been reported using Geotail data (Kojima et al., 1997). However, these Geotail observations are from the distant magnetosheath (> 30 R_E) whereas Cluster's are from near Earth (< 19.5 R_E). Unlike the typical tens of microsecond time durations of the bipolar solitary waves observed on Cluster, the typical time duration on Geotail for these solitary waves was 1 - 2 milliseconds. Although we have no way of knowing since Cluster's orbit does not transit the distant magnetosheath, there is the possibility that the limited bandwidth of the Geotail waveform capture instrument prevented the measurement of the shorter time duration bipolar pulses that are typical of the near-Earth magnetosheath as observed by Cluster. Kojima et al. (1997) suggested that since the solitary waves observed in the magnetosheath had a similar nature to those observed in the plasma sheet boundary layer and since those in the latter seem to be explained by electron dynamics only, the magnetosheath solitary waves could probably be explained as well in terms of electron dynamics only.

Jovanović and Shukla (2002, 2004) have proposed a nonlinear model that provides a theoretical explanation for some of the electrostatic and weakly electromagnetic bipolar structures that have been observed in Earth's magnetosheath, as well as at the magnetopause and in the auroral zone. This mode is based on a drift-kinetic theory for electron phase-space vortices in magnetized space plasmas formulated in the frequency range of the lower-hybrid waves excited by the Buneman instability in the presence of an electron beam. This model accounts for the effects of the electron polarization, anisotropic electron temperature and ion mobility. The quasi-3-D electron holes have the form of either elongated cylinders oblique to the magnetic field, or spheroids. Chen et al. (2004) have proposed a theory for understanding the ubiquity of solitary waves observed in different classes of collisionless plasmas, including the solitary waves observed in the magnetosheath. They obtained trapped particle solutions for 3D BGK electron and ion solitary waves, taking into account dynamics of both species. They derived from the solutions exact inequality relations that constrain the widths and amplitudes of the solitary waves, and the temperature ratio between electrons and ions. They suggest that the continuum of allowed parameter space of BGK waves is responsible for their ubiquity.

Acknowledgments: Work at the University of Iowa was carried out under NASA/GSFC Grant NNG04GB98G.

References:

Chen, L.-J and G. D. Parks, BGK electron solitary waves in 3D magnetized plasma, Geophys. Re. Lett., 29(9), 10.1029/2001GL013385, 2002a.

Chen, L.-J. and G. D. Parks, BGK electron solitary waves: 1D and 3D, Nonlin. Proc. Geophys., 9, 111, 2002b.

Chen, L.-J., D. J. Thouless, and J.-M. Tang, Bernstein-Greene-Kruskal solitary waves in three-dimensional magnetized plasma, Phys. Rev. E, 69, 055402(R), 2004.

Dupree, T. H., Large amplitude ion holes, Phys. Fluids, 29, 1820, 1986.

Ergun, R. E., C. W. Carlson, J. P. McFadden, F. S. Mozer, L. Muschietti, I. Roth, and R. J. Strangeway, Debye-scale plasma structures associated with magnetic-field-aligned electric fields, Phys. Rev. Lett., 81, 826, 1998.

Franz, Jason Richard, A Study of Electron Phase-Space Holes in the Polar Magnetosphere, Ph.D. Dissertation, Cornell University, Ithaca, NY, 2000

J. A. Franz, P. M. Kintner, and J. S. Pickett, Polar observations of coherent electric field structures, Geophys. Res. Lett., 25, 1277,1998.

Franz, J. A., P. M. Kintner, C. E. Seyler, J. S. Pickett, and J. D. Scudder, On the perpendicular scale of electron phase-space holes, Geophys. Res. Lett., 27, 169, 2000.

Goldstein, M. L., P. Decreau, J. Eastwood, E. A. Lucek, J. Pickett and R. Treumann, Chapter 1: The Near Earth Solar Wind, in "Dayside Magnetospheric Boundaries: Cluster Results", ISSI Space Science Series, Volume 20, Bern, Switzerland, 2005.

Gurnett, D. A., et al., The Polar Plasma Wave Instrument, Space Sci. Rev., 71, 597, 1995.

Jovanović, D, P. K. Shukla, L. Stenflo, and F. Pegoraro, Nonlinear model for electron phase-space holes in magnetized space plasmas, J. Geophys. Res., 107, No. A7, 10.1029/2001JA900180, 2002.

Jovanović, D. and P. K. Shukla, Solitary waves in the Earth's magnetosphere: Nonlinear stage of the lower-hybrid Buneman instability, Geophys. Res. Lett., 31, L05805, doi:10.1029/2003GL018047, 2004.

Kojima, H., H. Matsumoto, S. Chikuba, S. Horiyama, M. Ashour-Abdalla, and R. R. Anderson, Geotail waveform observations of braodband/narrowband electrostatic noise in the distant tail, J. Geophys. Res., 201, No. A7, 14,439, 1997.

Krasovsky, V. L., H. Matsumoto, and Y. Omura, Bernstein-Greene-Kruskal analysis of electrostatic solitary waves observed with Geotail, J. Geophys. Res., 102, 22131, 1997.

Mangeney, A., C. Salem, C. Lacombe, J.-L. Bougeret, C. Perche, et al: WIND observations of coherent electrostatic waves in the solar wind, Annales Geophys., 17, 307, 1999.

Pickett, J. S., J. R. Franz, J. D. Scudder, J. D. Menietti, D. A. Gurnett, G. B. Hospodarsky, R. M. Braunger, P. M. Kintner, and W. S. Kurth, Plasma waves observed in the cusp turbulent boundary layers: An analysis of high time resolution wave and particle measurements from the Polar spacecraft, J. Geophys. Res., 106, 19081, 2001.

Pickett, J. S., J. D. Menietti, D. A. Gurnett, B. Tsurutani, P. M. Kintner, E. Klatt, and A. Balogh, Solitary potential structures observed in the magnetosheath by the Cluster spacecraft, Nonlin. Proc. Geophys., 10, 3, 2003.

Pickett, J. S., S. W. Kahler, L.-J.Chen, R. L. Huff, O. Santolik, Y. Khotyaintsev, P. M. E. Decreau, D. Winningham, R. Frahm, M. L. Goldstein, G. S. Lakhina, B. T. Tsurutani, B. Lavraud, D. A. Gurnett, M. Andre, A. Fazakerley, A. Balogh, and H. Reme, Solitary waves observed in the auroral zone: the Cluster multi-spacecraft perspective, Nonlin. Proc. Geophys., 11, 183, 2004a.

Muschietti, L., I. Roth, C. W. Carlson, and M. Berthomier, Modeling stretched solitary waves along magnetic field lines, Nonlin. Proc. Geophys. 9, 101, 2002.

Pickett, J., S., L.-J.Chen, S. w. Kahler, O. Santolik, D. A. Gurnett, B. T. Tsurutani, and A. Balogh, Isolated electrostatic structures observed throughout the Cluster orbit: relationship to magnetic field strength, Annales Geophys., 22, 2515, 2004b.

Pickett, J. S., L.-J. Chen, S. W. Kahler, O. Santolik, M. L. Goldstein, B. Lavraud, P. M. Decreau, R. Kessel, E. Lucek, G. S. Lakhina, B. T. Tsurutani, D. A. Gurnett, N. Cornilleau-Wehrlin, a. Fazakerley, H. Reme, and A. Balogh, On the generation of solitary waves observed by Cluster in the Near-Earth Magnetosheath, Nonlin. Proc. Geophys., in press, 2005.

Scudder, J., et al., HYDRA: A 3-dimensional electron and ion hot plasma instrument for the Polar spacecraft of the GGS mission, Space. Sci. Rev., 71, 459, 1995.

Table 1 Properties of the coherent structures detected in the cusp and plasma sheet by Polar PWI (adapted from Franz, 2000)

	Cusp	Plasma Sheet
Number detected by automatic algorithm	2836	1260
Number for which velocity is resolvable	27% (769)	40% (496)
Velocity, V: $V < V_e$ $V > V_{IA\_soliton}$ V_{avg} V > 3614 km/s	 61%-65% > 95% 870 km/s 27%	 60% - 99% > 74% > 3614 km/s 99%

Parallel Scale Size, $L_{//}$:
$L_{//} > \lambda_D$
Typical $L_{//}$
	
	80% - 89%
	several 10s of meters (4% > 400 m)
		
		35% - 55%
		few 100s of meters (84% > 300 m)

Amplitude, $E_{//}$:
Typical $E_{//}$
$e\varphi/k_B T_e << 1$
	
	< 1 mV/m
	100%
		
		< 1 mV/m
		100%

Shape	Pancake-like: 80% have $\|E_\perp/E_{//}\| < 0.45$	Spherical: 80% have $\|E_\perp/E_{//}\| < 1.15$

Figure 1: Cluster cross-spacecraft correlation of tripolar pulses observed on 6 April 2002 around 10:36:06 UT in the auroral zone at about 4.8 R_E. Panels (A) and (B) show the calibrated waveforms from SC1 and SC3, respectively. Panel (C) shows the correlation coefficient reaching almost 0.8 at about 10 data point lags. Panel (D) shows the waveform from SC1 overplotted on SC3 after applying the appropriate lag to SC1. Note that the initial large tripolar pulse and the last smaller amplitude pulse nicely line up with each other. Although the initial tripolar pulse in SC1 is "clipped", the receiver is not in saturation so that it provides a valid time duration and form. (From Pickett et al., 2004a)

Figure 2: Scatter plots of the relationships between the (normalized) structure properties in the cusp. These plots show a trend for larger scale structures to have larger velocities (panel 1), larger amplitude structures to have larger velocities (panel 3) and larger scale structures to have larger amplitudes (panel 2). (From Franz, 2000)

Figure 3: Survey of the bipolar pulses observed by Cluster WBD over a two-year period showing the electric field amplitude vs. magnetic field strength. A trend of increasing electric field amplitude with increasing magnetic field strength is observed. The over plotted bracketed lines with an imbedded "x" within each regional grouping represent the standard deviation and mean of that group, respectively. (From Pickett et al., 2004b)

Figure 4: Characteristics (peak-to-peak amplitude in top panel and pulse duration in bottom panel) of the solitary waves observed during the survey interval as a function of distance from the bow shock, in R_E. Note that 0 R_E is the location of the model bow shock, with positive distances lying downstream in the magnetosheath. The points that appear to lie upstream of the bow shock are actually downstream and a consequence of the model not being able to predict the bow shock location to better than 1 R_E. There is no change in either the amplitude or time duration of the solitary waves as the spacecraft get farther from the bow shock, implying that the structures are generated locally in the magnetosheath. (From Pickett et al., 2005)

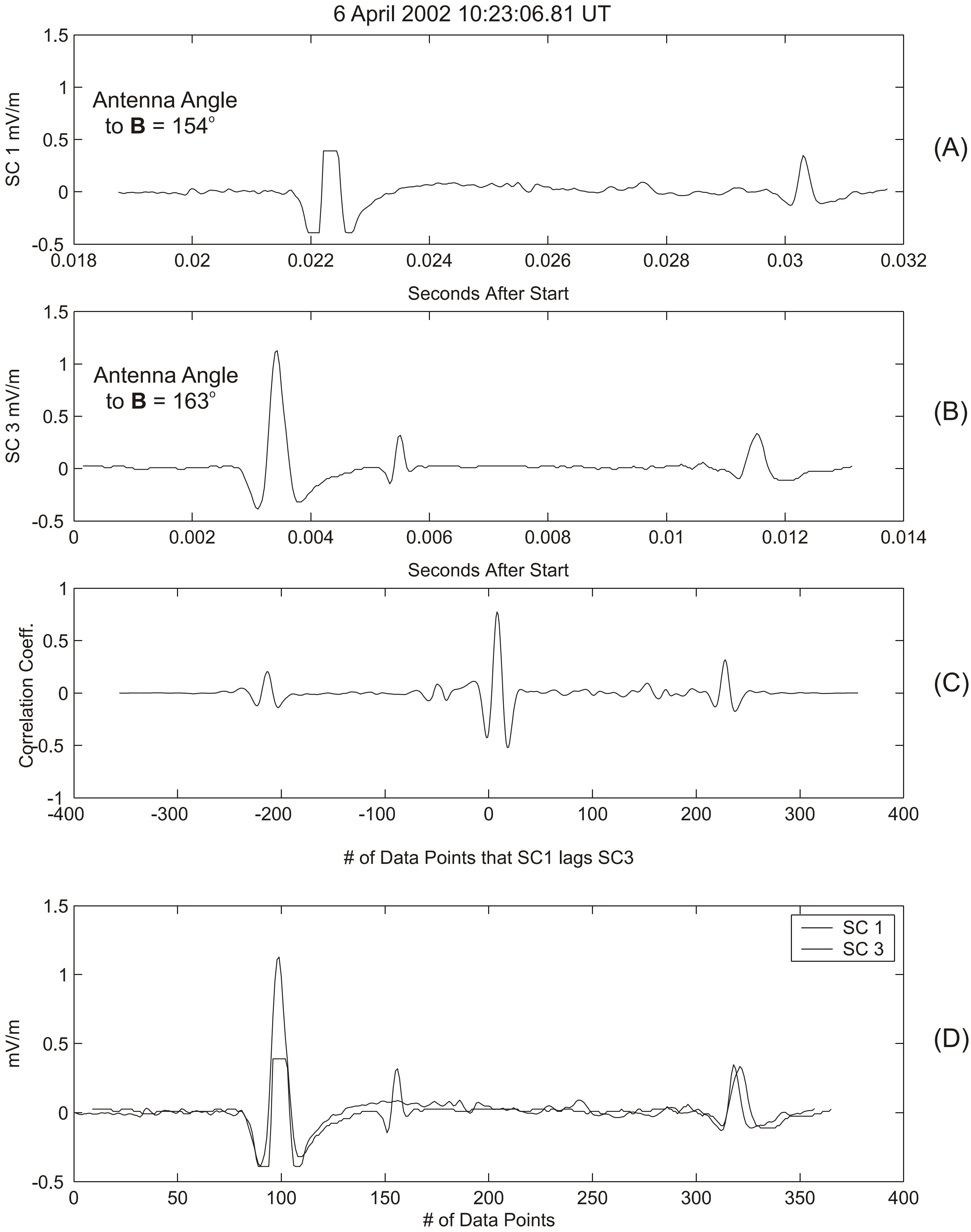
6 April 2002 10:23:06.81 UT
Antenna Angle
to **B** = 154°
SC 1 mV/m
Seconds After Start
(A)
Antenna Angle
to **B** = 163°
SC 3 mV/m
Seconds After Start
(B)
Correlation Coeff.
# of Data Points that SC1 lags SC3
(C)
SC 1
SC 3
mV/m
# of Data Points
(D)

Figure 1

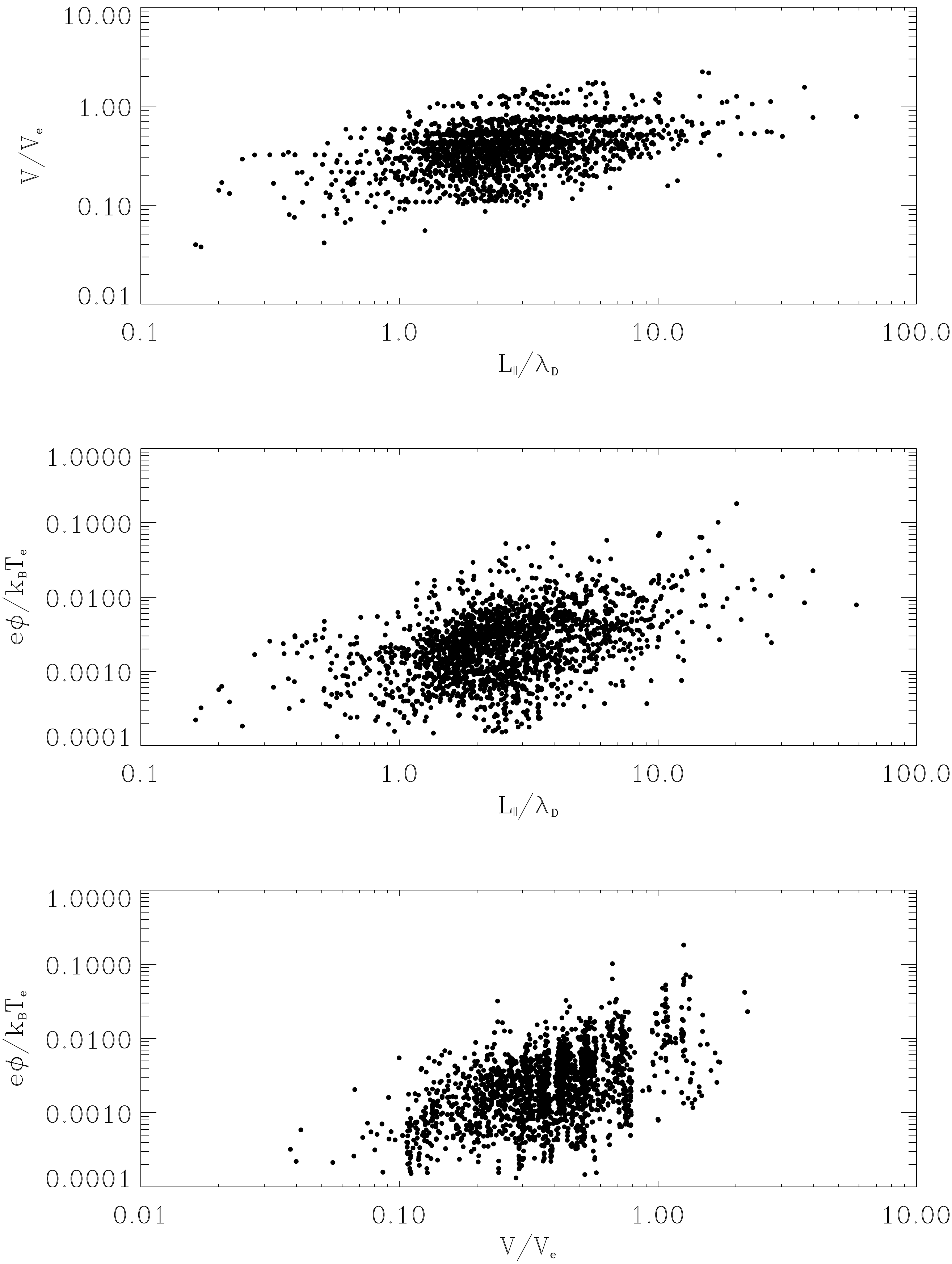

10.00
1.00
0.10
0.01
V/V$_e$
0.1
1.0
10.0
100.0
L$_\parallel$/λ$_D$
1.0000
0.1000
0.0100
0.0010
0.0001
eφ/k$_B$T$_e$
0.1
1.0
10.0
100.0
L$_\parallel$/λ$_D$
1.0000
0.1000
0.0100
0.0010
0.0001
eφ/k$_B$T$_e$
0.01
0.10
1.00
10.00
V/V$_e$

Figure 2

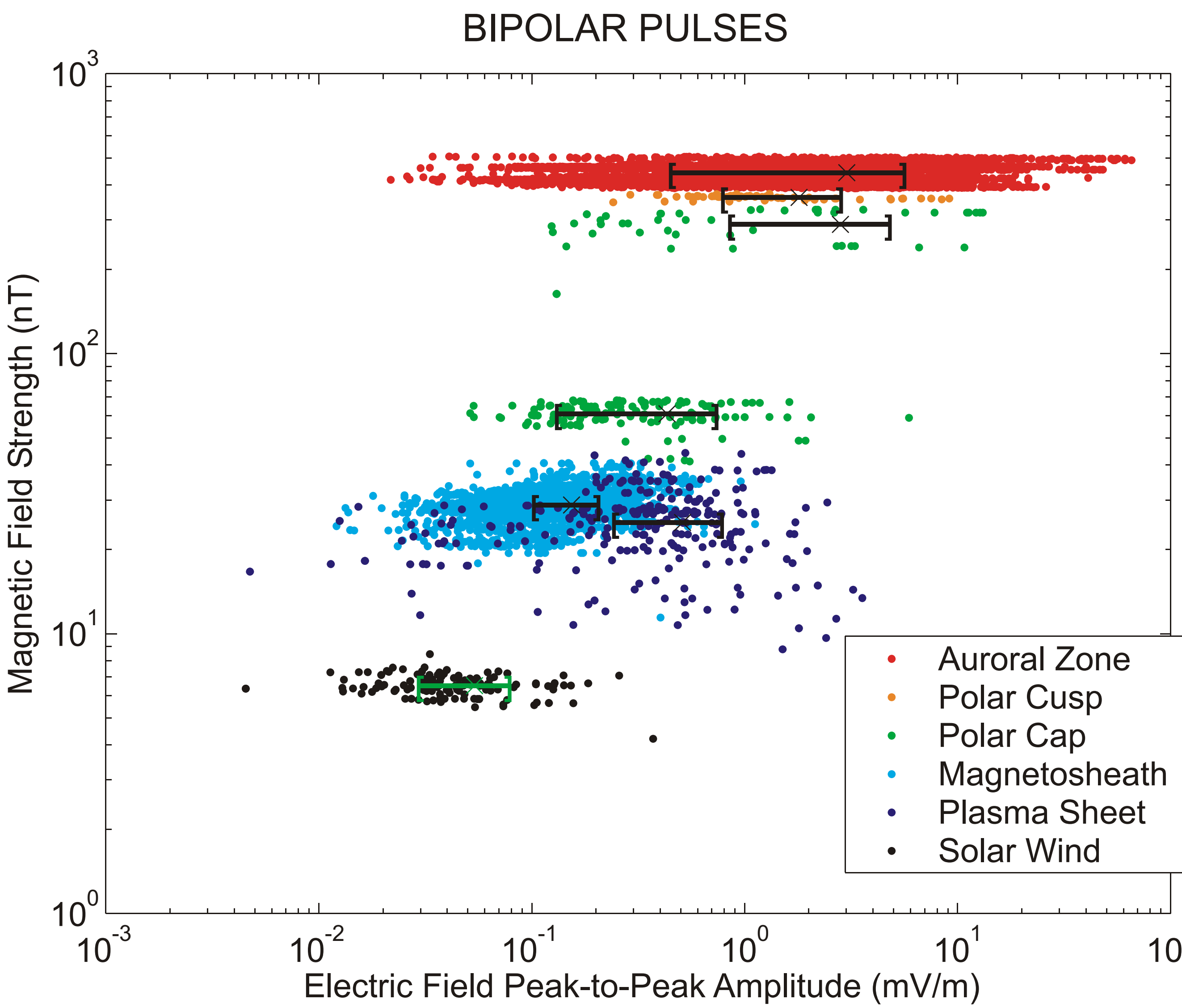
BIPOLAR PULSES
Magnetic Field Strength (nT)
Electric Field Peak-to-Peak Amplitude (mV/m)
10^3
10^2
10^1
10^0
10^-3
10^-2
10^-1
10^0
10^1
10^2
Auroral Zone
Polar Cusp
Polar Cap
Magnetosheath
Plasma Sheet
Solar Wind

Figure 3

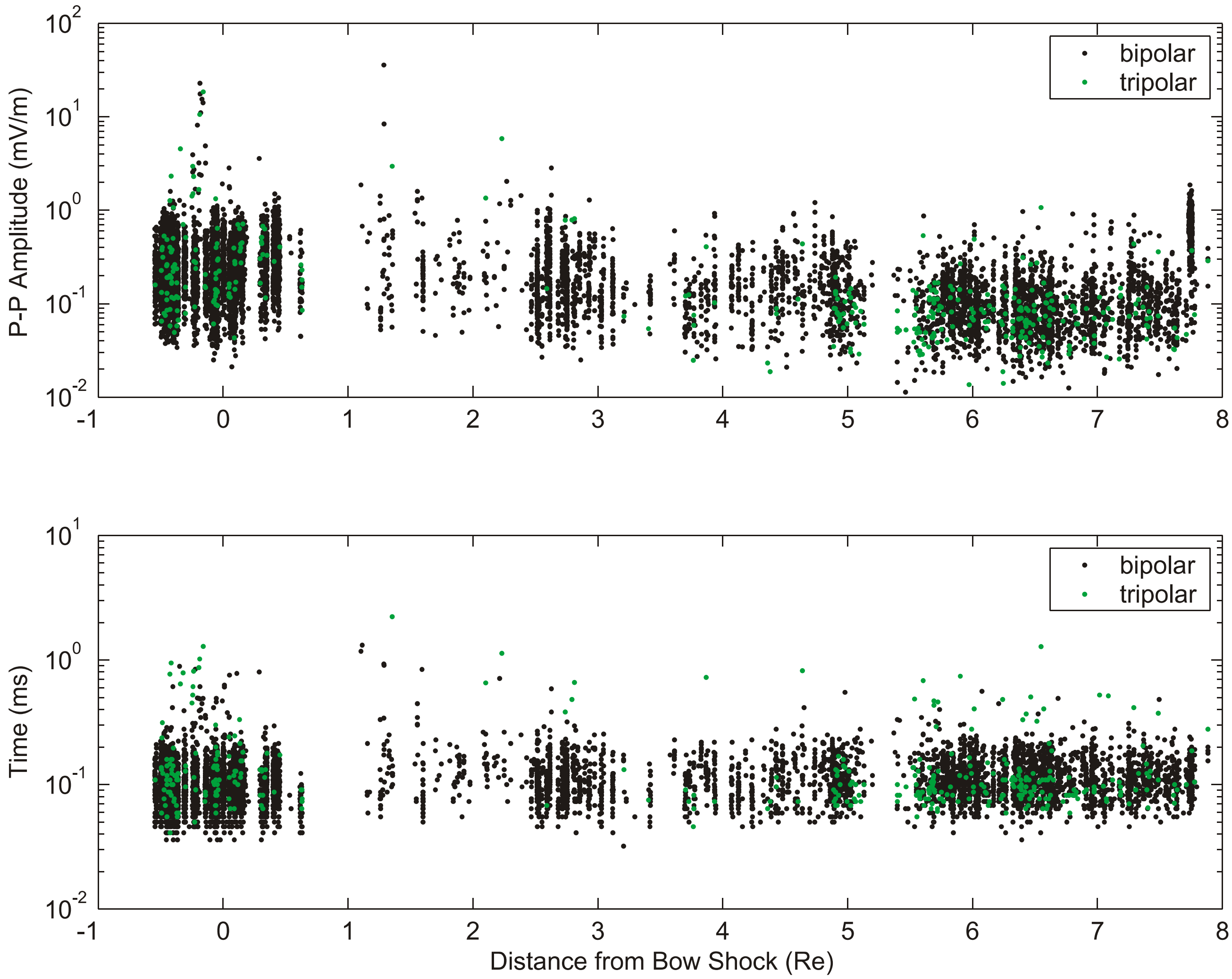

P-P Amplitude (mV/m)
10^{2}
10^{1}
10^{0}
10^{-1}
10^{-2}
bipolar
tripolar
Time (ms)
10^{1}
10^{0}
10^{-1}
10^{-2}
-1
0
1
2
3
4
5
6
7
8
Distance from Bow Shock (Re)

Figure 4